Spontaneous emission in stimulated Raman adiabatic passage

P. A. Ivanov,[1] N. V. Vitanov,[1,2] and K. Bergmann[3]
[1]*Department of Physics, Sofia University, James Bourchier 5 blvd, 1164 Sofia, Bulgaria*
[2]*Institute of Solid State Physics, Bulgarian Academy of Sciences, Tsarigradsko chaussée 72, 1784 Sofia, Bulgaria*
[3]*Fachbereich Physik der Universität, Erwin-Schrödinger-Str., 67653 Kaiserslautern, Germany*
(Received 29 July 2005; published 18 November 2005)

This work explores the effect of spontaneous emission on the population transfer efficiency in stimulated Raman adiabatic passage (STIRAP). The approach uses adiabatic elimination of weakly coupled density matrix elements in the Liouville equation, from which a very accurate analytic approximation is derived. The loss of population transfer efficiency is found to decrease exponentially with the factor Ω_0^2/Γ, where Γ is the spontaneous emission rate and Ω_0 is the peak Rabi frequency. The transfer efficiency increases with the pulse delay and reaches a steady value. For large pulse delay and large spontaneous emission rate STIRAP degenerates into optical pumping.

DOI: 10.1103/PhysRevA.72.053412 PACS number(s): 32.80.Bx, 33.80.−b, 33.80.Be

I. INTRODUCTION

Stimulated Raman adiabatic passage (STIRAP) [1–4] is a simple and powerful technique for complete and robust population transfer in three-state quantum systems. In this techique, the population is transferred adiabatically from an initially populated state $|1\rangle$ to a target state $|3\rangle$, which are coupled via an intermediate state $|2\rangle$ by two pulsed fields, pump and Stokes. Quite a remarkable and unique feature of STIRAP is that during the transfer the population remains trapped in a dark state $|d(t)\rangle$, which is a time-dependent superposition of states $|1\rangle$ and $|3\rangle$ only and does not involve the intermediate state $|2\rangle$. Such a dark state is formed by maintaining the two-photon resonance between states $|1\rangle$ and $|3\rangle$. If the pulses are ordered counterintuitively, the Stokes before the pump, then state $|d(t)\rangle$ is associated with state $|1\rangle$ initially and state $|3\rangle$ in the end, thus providing an adiabatic route from $|1\rangle$ to $|3\rangle$.

Real physical systems are rarely perfect. Real atoms and molecules can be exposed to various decoherence effects, such as phase relaxation (dephasing) and population losses due to spontaneous emission or ionization.

Losses from the intermediate state $|2\rangle$ to other states out of the system are treated relatively easily because one can use the Schrödinger equation and model the losses by including an imaginary decay rate in the Hamiltonian [5]. In the adiabatic limit state $|2\rangle$ never gets populated and its decay is irrelevant. However, if the decay rate becomes sufficiently large then adiabaticity breaks down and the transfer efficiency of STIRAP decreases [5].

Phase relaxation is a more subtle effect, as far as STIRAP is concerned, because its effect is indirect: it destroys the coherence between states $|1\rangle$ and $|3\rangle$, which leads to depopulation of the dark state $|d(t)\rangle$ and subsequent loss of efficiency [6–8]. Recently, we have provided an analytic description of the dephasing effects on STIRAP and we have derived simple analytic estimates of the transfer efficiency [8]. Treating dephasing is more difficult than population loss because it requires the use of the density-matrix Liouville equation, which is considerably more complex than the Schrödinger equation.

We also mention another very recent work, where instead of trying to avoid population decay, STIRAP has been used in a ladder system to steer the population flow out of the system, that is to enhance fluorescence from state $|3\rangle$ and suppress that from state $|2\rangle$ [9].

In this paper, we present an analytic description of STIRAP in the presence of spontaneous emission from the intermediate state to the other two states *within* a Λ system. This problem is considerably more difficult than the description of losses to states outside the system or dephasing because spontaneous emission occurs from a state, which is *unpopulated* in the adiabatic limit; hence one cannot use the adiabatic solution of the Liouville equation in this case. We derive the solution by using a dark-excited-bright basis and by adiabatically eliminating all weakly coupled populations and coherences. We provide an example of the general solution in the case of Gaussian pulse shapes.

This paper is organized as follows. In Sec. II we provide background knowledge of STIRAP and define the problem. We derive the solution of the Liouville equation in Sec. III for equal decay rates to states $|1\rangle$ and $|3\rangle$. We then compare this solution to numerical simulations in Sec. IV. The effects of unequal decay rates are discussed in Sec. V. A summary is presented in Sec. VI.

II. GENERAL BACKGROUND

A. The three-state system

The interaction of the three-state Λ system with the laser fields is described, in the rotating-wave approximation [10], by the Hamiltonian

$$\mathsf{H}(t) = \frac{\hbar}{2}\begin{bmatrix} 0 & \Omega_p(t) & 0 \\ \Omega_p(t) & 2\Delta(t) & \Omega_s(t) \\ 0 & \Omega_s(t) & 0 \end{bmatrix}. \tag{1}$$

The Λ system is shown in Fig. 1(a). A two-photon resonance between states $|1\rangle$ and $|3\rangle$ is maintained while state $|2\rangle$ can be generally off resonance by a certain detuning Δ. For simplicity, we assume a single-photon resonance,

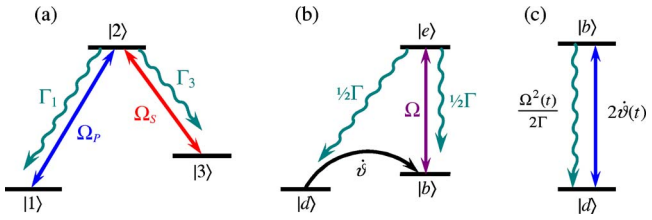

FIG. 1. (Color online) (a) The three-state Λ system studied in this paper in the original basis. (b) The Λ system in the bright-excited-dark basis for equal decay rates, $\Gamma_1=\Gamma_3=\frac{1}{2}\Gamma$. (c) The effective two-state system after adiabatic elimination of weakly coupled density matrix elements.

$$\Delta = 0; \tag{2}$$

the detuning effects have been discussed elsewhere [11].

The functions $\Omega_p(t)$ and $\Omega_s(t)$ in Eq. (1) are the Rabi frequencies of the pump and Stokes pulses, respectively, and each of them is proportional to the electric-field amplitude of the respective laser field and the corresponding transition dipole moment, $\Omega_p(t)=-\mathbf{d}_{12}.\mathbf{E}_p(t)/\hbar$ and $\Omega_s(t)=-\mathbf{d}_{32}.\mathbf{E}_s(t)/\hbar$. Without loss of generality both $\Omega_p(t)$ and $\Omega_s(t)$ will be assumed real and positive as the populations do not depend on their phases.

STIRAP proceeds through the dark (or trapped) state,

$$|d(t)\rangle = \frac{\Omega_s(t)}{\Omega(t)}|1\rangle - \frac{\Omega_p(t)}{\Omega(t)}|3\rangle, \tag{3}$$

where

$$\Omega(t) = \sqrt{\Omega_p(t) + \Omega_s(t)} \tag{4}$$

is the rms Rabi frequency. This state is an eigenstate (adiabatic state) of the Hamiltonian (1), with a zero eigenvalue, and it is a time-dependent coherent superposition of states $|1\rangle$ and $|3\rangle$. In STIRAP the pulses are applied in the *counterintuitive* order, i.e., the Stokes pulse $\Omega_s(t)$ precedes the pump pulse $\Omega_p(t)$; then

$$\lim_{t\to-\infty}\frac{\Omega_p(t)}{\Omega_s(t)} = 0, \quad \lim_{t\to\infty}\frac{\Omega_p(t)}{\Omega_s(t)} = \infty. \tag{5}$$

Consequently, the dark state $|d(t)\rangle$ is equal to state $|1\rangle$ as $t\to-\infty$ and to state $-|3\rangle$ as $t\to\infty$. If the evolution is adiabatic, which requires large pulse area [4], then the system remains in the dark state $|d(t)\rangle$ at all times and the population is transferred completely to state $|3\rangle$.

A unique feature of STIRAP is that in the adiabatic limit the intermediate state $|2\rangle$ remains unpopulated, even transiently, because the dark state $|d\rangle$ does not involve it. This feature makes STIRAP robust against population relaxation effects, such as spontaneous emission from state $|2\rangle$ within the system or irreversible loss from state $|2\rangle$ to levels outside the system. State $|2\rangle$ can get some population only if the evolution is not perfectly adiabatic; then it will decay and the transfer efficiency of STIRAP will decrease. Hence, in order to describe the effect of spontaneous emission from state $|2\rangle$ within the system we cannot use the adiabatic approximation and have to account for the nonadiabatic couplings.

B. The Liouville equation

1. Diabatic basis

We model the effect of relaxation processes on quantum dynamics by introducing phenomenological decay terms into the Liouville equation,

$$i\hbar\dot{\rho} = [\mathsf{H},\rho] + \mathsf{D}, \tag{6}$$

where an overdot means d/dt. The dissipator D describes spontaneous emission within the system,

$$\mathsf{D}(t) = -i\frac{\hbar}{2}\begin{bmatrix} -2\Gamma_1\rho_{22} & (\Gamma_1+\Gamma_3)\rho_{12} & 0 \\ (\Gamma_1+\Gamma_3)\rho_{21} & 2(\Gamma_1+\Gamma_3)\rho_{22} & (\Gamma_1+\Gamma_3)\rho_{23} \\ 0 & (\Gamma_1+\Gamma_3)\rho_{32} & -2\Gamma_3\rho_{22} \end{bmatrix}, \tag{7}$$

with Γ_1 and Γ_3 being constant rates of spontaneous emission from the exited state $|2\rangle$ to states $|1\rangle$ and $|3\rangle$, respectively. Equation (6) is solved with the condition that the system is initially in state $|1\rangle$,

$$\rho_{11}(-\infty) = 1, \quad \rho_{mn}(-\infty) = 0 \quad (mn \neq 11). \tag{8}$$

In terms of the parameters

$$\Gamma = \Gamma_1 + \Gamma_3, \quad \gamma = \Gamma_1 - \Gamma_3, \tag{9}$$

the dissipator (7) reads

$$\mathsf{D}(t) = \mathsf{D}_\Gamma(t) + \mathsf{D}_\gamma(t), \tag{10a}$$

$$\mathsf{D}_\Gamma(t) = -i\hbar\frac{\Gamma}{2}\begin{bmatrix} -\rho_{22} & \rho_{12} & 0 \\ \rho_{21} & 2\rho_{22} & \rho_{23} \\ 0 & \rho_{32} & -\rho_{22} \end{bmatrix}, \tag{10b}$$

$$\mathsf{D}_\gamma(t) = i\hbar\frac{\gamma}{2}\begin{bmatrix} \rho_{22} & 0 & 0 \\ 0 & 0 & 0 \\ 0 & 0 & -\rho_{22} \end{bmatrix}. \tag{10c}$$

We first assume that the two decay rates are equal,

$$\Gamma_1 = \Gamma_3 = \frac{1}{2}\Gamma, \tag{11}$$

which means that $\gamma=0$, $\mathsf{D}_\gamma(t)=0$ and $\mathsf{D}(t)=\mathsf{D}_\Gamma(t)$; this greatly simplifies the treatment. For example, such a situation occurs when STIRAP is realized between the magnetic sublevels $m=-1$ and $m=1$ of a $J=1$ level via the sublevel $m=0$ of a $J=0$ or $J=1$ level by two left and right circularly polarized laser pulses [4]. In Sec. V we shall discuss the effects of unequal Γ_1 and Γ_3.

2. Bright-excited-dark basis

We choose a basis composed of the dark state $|d(t)\rangle$, the bright state $|b(t)\rangle$, and the excited state $|e\rangle$,

$$|b(t)\rangle = \sin\vartheta(t)|1\rangle + \cos\vartheta(t)|3\rangle, \tag{12a}$$

$$|e\rangle = |2\rangle, \tag{12b}$$

$$|d(t)\rangle = \cos\vartheta(t)|1\rangle - \sin\vartheta(t)|3\rangle, \tag{12c}$$

where the mixing angle $\vartheta(t)$ is defined by

$$\tan\vartheta(t) = \frac{\Omega_p(t)}{\Omega_s(t)}. \tag{13}$$

There are several reasons for this choice of basis instead of the traditional adiabatic basis. The presence of the dark state $|d(t)\rangle$ is a must, as far as STIRAP is concerned, because it is this state where the population resides entirely in the adiabatic limit in the absence of decoherence; our solution should reduce to the lossless solution for $\Gamma=0$ and therefore, the dark state must be in the basis. The decaying state $|e\rangle$ is chosen as another basis state, which is justified by its special role as the only decaying state, which makes it distinctly different from states $|1\rangle$ and $|3\rangle$, or any linear superposition of them. Had we chosen to work in the adiabatic basis instead, then we would have to deal with two adiabatic states (besides the dark state), which are superpositions of all bare states $|1\rangle$, $|2\rangle$, and $|3\rangle$, and hence they involve both decaying and stable states, which complicates the treatment. Finally, once we have chosen states $|d(t)\rangle$ and $|e\rangle$ for the new basis, they determine the third state $|b(t)\rangle$ uniquely (up to an unimportant global sign).

The vectors (12) form the matrix ($\mathsf{R}^{-1}=\mathsf{R}$)

$$\mathsf{R}(t) = \begin{bmatrix} \sin\vartheta(t) & 0 & \cos\vartheta(t) \\ 0 & 1 & 0 \\ \cos\vartheta(t) & 0 & -\sin\vartheta(t) \end{bmatrix}, \tag{14}$$

which transforms the Liouville equation in the new basis,

$$i\hbar\dot{\tilde{\rho}} = [\widetilde{\mathsf{H}},\tilde{\rho}] - i\hbar[\mathsf{R}\dot{\mathsf{R}},\tilde{\rho}] + \widetilde{\mathsf{D}}, \tag{15}$$

where

$$\tilde{\rho} = \mathsf{R}\rho\mathsf{R}, \tag{16a}$$

$$\widetilde{\mathsf{H}} = \mathsf{RHR} = \frac{\hbar}{2}\begin{bmatrix} 0 & \Omega(t) & 0 \\ \Omega(t) & 0 & 0 \\ 0 & 0 & 0 \end{bmatrix}, \tag{16b}$$

$$\widetilde{\mathsf{D}} = \mathsf{RDR} = -i\hbar\frac{\Gamma}{2}\begin{bmatrix} -\rho_{ee} & \rho_{be} & 0 \\ \rho_{eb} & 2\rho_{ee} & \rho_{ed} \\ 0 & \rho_{de} & -\rho_{ee} \end{bmatrix}. \tag{16c}$$

The linkage pattern in this basis is sketched in Fig. 1(b). In this basis the excited state $|e\rangle$ decays to the dark and bright states $|d\rangle$ and $|b\rangle$ with the same rates $\Gamma/2$ as to states $|1\rangle$ and $|3\rangle$ in the original basis.

Equation (15) is solved with the initial conditions

$$\rho_{dd}(-\infty) = 1, \quad \rho_{\mu\nu}(-\infty) = 0 \quad (\mu\nu \neq dd). \tag{17}$$

The transformed Liouville equation (15) still involves nine coupled differential equations, as the original Eq. (6). Using $\mathrm{Tr}\,\tilde{\rho}=1$ the system reduces to eight equations, but the problem remains unsoluble exactly. However, the advantage of the new basis is that it allows one to make some reasonable approximations, which reduce the problem considerably, to a soluble one. The approximate solution of Eq. (15) is derived in the next section.

III. STIRAP AMIDST SPONTANEOUS EMISSION

A. Irrelevance of adiabatic evolution assumption

In the adiabatic approximation, one neglects the nonadiabatic coupling term $-i\hbar[\mathsf{R}\dot{\mathsf{R}},\tilde{\rho}]$ in the Liouville equation (15), which is $\propto\dot{\vartheta}$. Then the solution does not depend on the decay rate Γ at all. Indeed, from Eq. (15) we find that in the adiabatic limit,

$$\begin{bmatrix} \mathrm{Im}\,\dot{\rho}_{be} \\ \dot{\rho}_{bb} \\ \dot{\rho}_{ee} \end{bmatrix} = \begin{bmatrix} -\frac{1}{2}\Gamma & \frac{1}{2}\Omega & -\frac{1}{2}\Omega \\ -\Omega & 0 & \frac{1}{2}\Gamma \\ \Omega & 0 & -\Gamma \end{bmatrix}\begin{bmatrix} \mathrm{Im}\,\rho_{be} \\ \rho_{bb} \\ \rho_{ee} \end{bmatrix}. \tag{18}$$

Equation (18) represents a system of linear homogeneous differential equations with null initial conditions (17); hence it has only the trivial solution

$$\rho_{ee}(t) = \rho_{bb}(t) = \mathrm{Im}\,\rho_{be}(t) = 0, \tag{19a}$$

from where it follows that

$$\rho_{dd}(t) = 1. \tag{19b}$$

The conclusion is that if the evolution is perfectly adiabatic then spontaneous emission does not affect STIRAP at all. The physical reason is that the lossy state $|e\rangle$ remains unpopulated in the adiabatic limit. Hence in order to determine the effect of spontaneous emission we *must* account for the nonadiabatic coupling between the dark state $|d\rangle$ and the bright state $|b\rangle$.

B. Adiabatic elimination of weakly coupled populations and coherences

We assume that the rms Rabi frequency is large compared to the nonadiabatic coupling,

$$\Omega(t) \gg |\dot{\vartheta}(t)|, \tag{20a}$$

which is the condition for adiabatic evolution in the absence of losses ($\Gamma=0$) [4], and we shall therefore consider $\dot{\vartheta}/\Omega$ as a small parameter. Furthermore, we assume that

$$\Gamma \gg \Omega_0, \tag{20b}$$

where Ω_0 is the peak Rabi frequency. The reason for this assumption is that for $\Gamma \lesssim \Omega_0$ the evolution is adiabatic and the solution is given by Eq. (19); decrease of transfer efficiency can only occur for condition (20b).

If the excited state $|e\rangle$ decays strongly then the density matrix elements involving this state change negligibly, $\dot{\rho}_{ee}=\dot{\rho}_{eb}=\dot{\rho}_{ed}\approx 0$, an assumption that amounts to adiabatic elimination of these elements. By inserting these derivatives into the Liouville equation (15), the corresponding three differential equations turn into algebraic equations, from which we determine ρ_{ee}, ρ_{eb}, and ρ_{ed} in terms of the other elements

of $\tilde{\rho}$: ρ_{bb}, ρ_{dd}, and ρ_{db} (the expressions are straightforward to derive but too cumbersome to be presented here).

By replacing ρ_{ee}, ρ_{eb}, and ρ_{ed} in the remaining differential equations for $\dot{\rho}_{bb}$, $\dot{\rho}_{dd}$, and $\dot{\rho}_{db}$ we find an effective reduced system of three linear differential equations involving ρ_{bb}, ρ_{dd}, and ρ_{db} and their derivatives only. In the next step, because of the assumptions (20) we neglect all terms of orders $O(\xi^2)$, $O(\eta^2)$, and $O(\xi\eta)$ and higher, where $\xi=\dot{\vartheta}/\Gamma$ and $\eta=\Omega/\Gamma$. Thus we obtain the relations

$$\mathrm{Re}\,\rho_{de} = -\frac{\Omega}{\Gamma}\,\mathrm{Im}\,\rho_{db} + O(\xi^2) + O(\xi\eta), \tag{21a}$$

$$\mathrm{Im}\,\rho_{de} = \frac{\Omega}{\Gamma}\,\mathrm{Re}\,\rho_{db} + O(\xi^2) + O(\xi\eta), \tag{21b}$$

$$\mathrm{Re}\,\rho_{be} = O(\xi^2) + O(\xi\eta), \tag{21c}$$

$$\mathrm{Im}\,\rho_{be} = \frac{\Omega}{\Gamma}\rho_{bb} + O(\xi^2) + O(\xi\eta) + O(\eta^2), \tag{21d}$$

$$\rho_{ee} = \frac{\Omega}{\Gamma}\left[\frac{\Omega}{\Gamma}\rho_{bb} + O(\xi^2) + O(\xi\eta) + O(\eta^2)\right]. \tag{21e}$$

The approximations (21) allow one to reduce Eq. (15) to just three equations,

$$\dot{u} = -\frac{\Omega^2}{2\Gamma}u, \tag{22a}$$

$$\dot{v} = -\frac{\Omega^2}{2\Gamma}v - 2\dot{\vartheta}w, \tag{22b}$$

$$\dot{w} = 2\dot{\vartheta}v - \frac{\Omega^2}{2\Gamma}(w+1), \tag{22c}$$

where $w=\rho_{bb}-\rho_{dd}$, $v=2\,\mathrm{Re}\,\rho_{db}$, and $u=2\,\mathrm{Im}\,\rho_{db}$, along with $\rho_{bb}(t)+\rho_{dd}(t)=1-O(\eta^2)$.

C. Approximate analytic solution

Equation (22) has exactly the same form as the Bloch equations for a two-state system [12], composed of states $|d\rangle$ and $|b\rangle$, which are coupled by a resonant field with a pulse-shaped coupling $2\dot{\vartheta}(t)$, and the bright state $|b\rangle$ "decays" spontaneously to the dark state $|d\rangle$ with a time-dependent rate $\Omega^2(t)/2\Gamma$. This effective two-state system is shown in Fig. 1(c). In this reduced picture, the spontaneous emission from state $|e\rangle$ in STIRAP shows up as "spontaneous emission" from state $|b\rangle$ to state $|d\rangle$; however, the rate $\Omega^2(t)/2\Gamma$ from state $|b\rangle$ is inversely proportional to the rate Γ from state $|e\rangle$. Hence the limit $\Gamma\to 0$ corresponds to an infinitely strong "spontaneous emission" $|b\rangle \rightsquigarrow |d\rangle$ resulting in population trapping in state $|d\rangle$. The limit $\Gamma\to\infty$ corresponds to absence of "spontaneous emission" from state $|b\rangle$, which results in lossless resonant excitation in the db system, with populations $P_d(t)=\cos^2\vartheta(t)$ and $P_b(t)=\sin^2\vartheta(t)$; since $\vartheta(\infty)=\pi/2$ [cf. Eq. (13)] we have $P_d(\infty)=0$, i.e., no population transfer at all.

The solution for Eq. (22a) is given immediately,

$$u = 2\,\mathrm{Im}\,\rho_{db}(t) = 0, \tag{23}$$

because Eq. (22a) is a linear homogeneous differential equation with a null initial condition. The other two equations (22b) and (22c) can be solved exactly and the time-dependent solution reads

$$\rho_{bb}(t) = e^{-f(t)}\int_{-\infty}^{t}\dot{\vartheta}(t')e^{f(t')}\sin[2\vartheta(t)-2\vartheta(t')]dt', \tag{24a}$$

$$\rho_{dd}(t) = 1-\rho_{bb}(t), \tag{24b}$$

where

$$f(t) = \frac{1}{2\Gamma}\int_{-\infty}^{t}\Omega^2(t')dt'. \tag{25}$$

By setting $\dot{\vartheta}(t)=0$, this solution reduces to the correct limit (19) for adiabatic evolution. The excited-state populaton (21e) is $\rho_{ee}(t)\sim O(\eta^2)\ll 1$.

D. Populations in the original basis

The time-dependent populations of states $|1\rangle$ and $|3\rangle$ can be determined from $\rho_{bb}(t)$ and $\rho_{dd}(t)$ by using Eq. (16a). Explicitly,

$$\rho_{11}(t) = \rho_{bb}(t)\sin^2\vartheta(t) + \rho_{dd}(t)\cos^2\vartheta(t) + \mathrm{Re}\,\rho_{bd}(t)\sin 2\vartheta(t), \tag{26a}$$

$$\rho_{33}(t) = \rho_{bb}(t)\cos^2\vartheta(t) + \rho_{dd}(t)\sin^2\vartheta(t) - \mathrm{Re}\,\rho_{bd}(t)\sin 2\vartheta(t). \tag{26b}$$

After the interaction, since $\vartheta(\infty)=\pi/2$, they are

$$\rho_{11}(\infty) = \rho_{bb}(\infty), \tag{27a}$$

$$\rho_{33}(\infty) = \rho_{dd}(\infty). \tag{27b}$$

Equations (26) and (27), with Eq. (24), provide the time-dependent and the final approximate solutions of the Liouville equation (6) in the presence of strong spontaneous emission, Eq. (20b).

E. Example: Gaussian pulses

We have performed numerical integration of the Liouville equation (6) for Gaussian pulses, with characteristic widths T, peak Rabi frequencies Ω_0, and delay τ,

$$\Omega_p(t) = \Omega_0 e^{-(t-\tau/2)^2/T^2}, \quad \Omega_s(t) = \Omega_0 e^{-(t+\tau/2)^2/T^2}. \tag{28}$$

For these pulses we have

$$\dot{\vartheta}(t) = \frac{\tau}{T^2}\,\mathrm{sech}\,\frac{2t\tau}{T^2}, \tag{29a}$$

$$f(t) = \sqrt{\frac{\pi}{2}}\frac{\Omega_0^2 T}{4\Gamma}\left[\mathrm{erf}\left(\frac{2t-\tau}{T\sqrt{2}}\right) + \mathrm{erf}\left(\frac{2t+\tau}{T\sqrt{2}}\right) + 2\right], \tag{29b}$$

where $\mathrm{erf}(x)$ is the error function [13]. The final populations (27) are given by

$$\rho_{11}(\infty) = \exp\left(-\sqrt{\frac{\pi}{2}}\frac{\Omega_0^2 T}{2\Gamma}\right)F, \tag{30a}$$

$$\rho_{33}(\infty) = 1 - \exp\left(-\sqrt{\frac{\pi}{2}}\frac{\Omega_0^2 T}{2\Gamma}\right)F, \tag{30b}$$

with

$$F = \frac{2\tau}{T^2}\int_0^\infty \mathrm{sech}^2\frac{2t\tau}{T^2}\cosh\left\{\sqrt{\frac{\pi}{2}}\frac{\Omega_0^2 T}{4\Gamma}\right.$$
$$\left.\times\left[\mathrm{erf}\left(\frac{2t-\tau}{T\sqrt{2}}\right) + \mathrm{erf}\left(\frac{2t+\tau}{T\sqrt{2}}\right)\right]\right\}dt, \tag{31}$$

where we have used $\mathrm{erf}(\infty)=1$. The integral (31) can be approximated as (see the Appendix)

$$F = \cosh a - \frac{\cosh a - 1}{\sqrt{b+1}}, \tag{32}$$

where

$$a = \frac{\Omega_0^2 T}{2\Gamma}\sqrt{\frac{\pi}{2}}, \tag{33a}$$

$$b = \frac{4a^2T^2e^{-\tau^2/T^2}}{\pi^2\tau^2(\cosh a - 1)}. \tag{33b}$$

Equation (30) provides the solution for the populations of the original diabatic states for Gaussian pulses (28) at the end of the interaction.

In the limit of no decay, $\Gamma \to 0$, we have

$$F \sim \frac{2a^2T^2e^{-\tau^2/T^2}}{\pi^2\tau^2}, \tag{34}$$

and hence Eq. (30) reduces to the correct STIRAP limit,

$$\rho_{11}(\infty) \underset{\Gamma\to 0}{\to} 0, \quad \rho_{33}(\infty) \underset{\Gamma\to 0}{\to} 1.$$

In the limit of very strong decay, $\Gamma \gg \Omega_0^2 T$, the integral (31) is approximated by

$$F \approx \frac{2\tau}{T^2}\int_0^\infty \mathrm{sech}^2\frac{2t\tau}{T^2}dt = 1, \tag{35}$$

and the solution for the populations reads

$$\rho_{11}(\infty) = \exp\left(-\sqrt{\frac{\pi}{2}}\frac{\Omega_0^2 T}{2\Gamma}\right), \tag{36a}$$

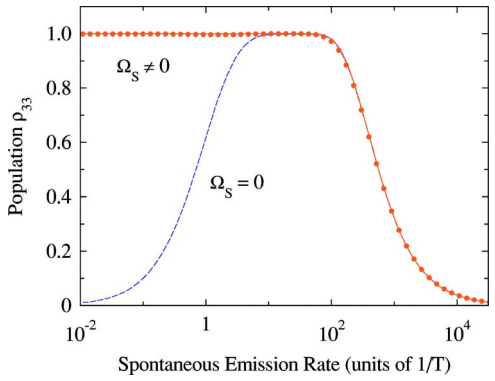

FIG. 2. (Color online) Final population ρ_{33} of state $|3\rangle$ as a function of the spontaneous emission rate Γ for Gaussian pulse shapes (28) with peak Rabi frequency $\Omega_0 = 25T^{-1}$ and delay $\tau = 1.5T$. The dots show the numerical solution of the Liouville equation (6) and the solid curve the analytic solution (36b). The dashed curve shows the numerical solution without the Stokes pulse, $\Omega_s(t) = 0$.

$$\rho_{33}(\infty) = 1 - \exp\left(-\sqrt{\frac{\pi}{2}}\frac{\Omega_0^2 T}{2\Gamma}\right). \tag{36b}$$

For $\Gamma \to \infty$, the populations tend to their unperturbed values,

$$\rho_{11}(\infty) \underset{\Gamma\to\infty}{\to} 1, \quad \rho_{33}(\infty) \underset{\Gamma\to\infty}{\to} 0,$$

which is a manifestation of *quantum overdamping*. The overdamping shows up as decoupling of the system from the driving fields; then the system freezes in its initial state. Curiously, Eq. (36) has also the correct $\Gamma \to 0$ limit,

$$\rho_{11}(\infty) \underset{\Gamma\to 0}{\to} 0, \quad \rho_{33}(\infty) \underset{\Gamma\to 0}{\to} 1.$$

It follows from Eq. (36b) that ρ_{33} decreases to $\frac{1}{2}$ for

$$\Gamma_{1/2}T = \frac{\sqrt{\pi/2}}{2\ln 2}(\Omega_0 T)^2. \tag{37}$$

Hence the range of Γ where high transfer efficiency is maintained, increases with the square of the pulse area.

IV. COMPARISON WITH NUMERICAL RESULTS

We have examined the validity of the analytic solution (30) by comparison with the numerical solution of the Liouville equation (6) for Gaussian pulse shapes (28). Figure 2 shows the final population of state $|3\rangle$ as a function of the spontaneous emission rate Γ from state $|2\rangle$ in two cases: with and without the Stokes pulse. In the presence of the Stokes pulse the population of state $|3\rangle$ shows considerable robustness for $\Gamma \lesssim 100T^{-1}$, which means that for this particular pulse area ($A = \Omega_0 T\sqrt{\pi} \approx 14\pi$) the excited state can decay up to 100 times during the population transfer without affecting the transfer efficiency. The approximate analytic solution (36b) is indistinguishable from the numerical values. For large decay rates, $\Gamma \gtrsim 100T^{-1}$, the population of state $|3\rangle$ departs from unity and decreases to zero for $\Gamma \to \infty$, as a result of overdamping. The value $\Gamma_{1/2}$ at which ρ_{33} decreases to $\frac{1}{2}$,

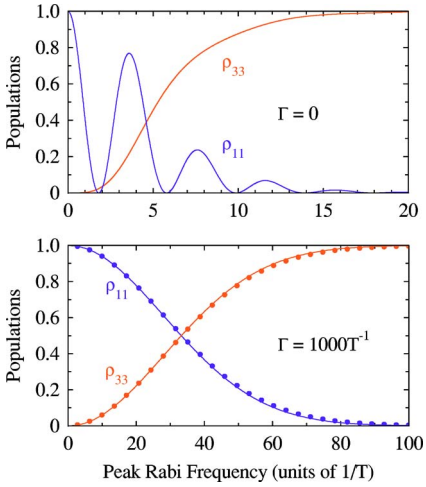

FIG. 3. (Color online) Final populations of states $|1\rangle$ and $|3\rangle$ against the peak Rabi frequency Ω_0 for Gaussian pulse shapes (28). The spontaneous emission rate is $\Gamma=0$ (upper frame) and $\Gamma=1000T^{-1}$ (lower frame) and the pulse delay is $\tau=1.5T$. In the upper frame the curves show numerical results. The dots in the lower frame show numeric results and the solid curves the analytic solution (36).

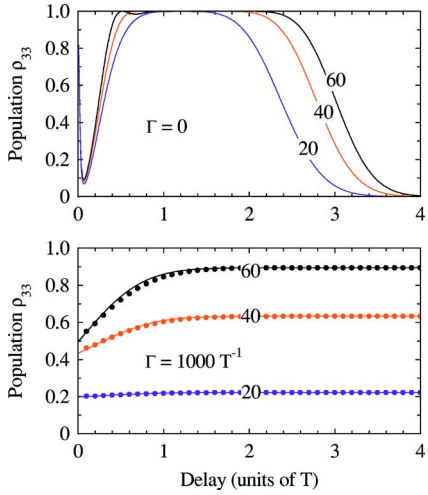

FIG. 4. (Color online) Final population ρ_{33} plotted against the pulse delay τ for Gaussian pulse shapes (28) with peak Rabi frequency $\Omega_0=20T^{-1}$, $40T^{-1}$, and $60T^{-1}$ (denoted on the respective curves). The spontaneous emission rate is $\Gamma=0$ (upper frame) and $\Gamma=1000T^{-1}$ (lower frame). In the upper frame the curves show numerical results. The dots in the lower frame show numerical results, whereas the curves show the analytic solution (30b) with the approximation (32).

Eq. (37), is $\Gamma_{1/2}\approx 565T^{-1}$, in excellent agreement with the numeric results.

In the absence of Stokes field ($\Omega_s=0$), the population of state $|3\rangle$ tends to zero for $\Gamma\to 0$, as should be the case because state $|3\rangle$ is uncoupled and population can only reach this state via (pulsed) optical pumping (OP). For weak-to-moderate spontaneous emission ($\Gamma T\lesssim 10$), it is STIRAP that transfers the population because the spontaneous emission rate is not high enough to enable OP. As Γ increases in the range $10\lesssim\Gamma T\lesssim 100$, the OP solution reaches unity and becomes indiscernible from the STIRAP solution. For $\Gamma T\gtrsim 100$, both STIRAP and OP are subjected to overdamping and $\rho_{33}\to 0$ for $\Gamma\to\infty$, as discussed above.

We emphasize that pulsed OP achieves the same result as STIRAP only because the system is closed. Moreover, the population transfer for $10\lesssim\Gamma T\lesssim 100$, dominated by OP, is incoherent, which implies that it is not accompanied by coherent momentum transfer.

Figure 3 shows the final populations against the peak Rabi frequency Ω_0. As Ω_0 increases adiabaticity improves and the populations reach their STIRAP values. An excellent agreement is observed between the analytic solution (36) and the numerical results. For comparison, the lossless solution is also plotted (upper frame), wherein the population ρ_{11} shows characterstic nonadiabatic oscillations. Figure 3 shows that although adiabaticity is deteriorated by spontaneous emission, meaning that high transfer efficiency requires higher Rabi frequencies, this effect is not very dramatic and the increase in the required Rabi frequency is only moderate.

In Fig. 4 the final population of state $|3\rangle$ is plotted as a function of the pulse delay τ in two cases: without (upper frame) and with spontaneous emission (lower frame). In the presence of spontaneous emission ρ_{33} increases as τ increases and reaches a steady value, which depends on the peak Rabi frequency Ω_0; this value is described very accurately by the analytic solution (30b). When τ is equal to just a few pulse widths ($\tau\sim 2.5T$), the lossless STIRAP (upper frame) breaks down due to deteriorated adiabaticity. In contrast, the transfer efficiency in the presence of spontaneous emission remains constant as τ increases indefinitely because beyond $\tau\sim 3T$ the population transfer dynamics is determined by OP, for which the delay is irrelevant.

V. EFFECT OF UNEQUAL DECAY RATES

Hitherto we have assumed that the decay rates from state $|2\rangle$ to states $|1\rangle$ and $|3\rangle$ are equal, Eq. (11). Different decay rates lead to the inclusion of the term D_γ, Eq. (10c), in the Liouville equation (6). By using again the dark-excited-bright basis and performing adiabatic elimination of density matrix elements involving the decaying excited state we obtain

$$\dot{v}=-\frac{\Omega^2}{2\Gamma}v-2\dot{\vartheta}w+\frac{\Omega^2\gamma\sin 2\vartheta}{2\Gamma^2}(w+1), \tag{38a}$$

$$\dot{w}=2\dot{\vartheta}v-\frac{\Omega^2}{2\Gamma}\left(1+\frac{\gamma\cos 2\vartheta}{\Gamma}\right)(w+1). \tag{38b}$$

We have verified by numeric integration that Eq. (38) provides virtually the same results as the full Liouville equation (15). Compared to Eq. (22), Eq. (38) has additional terms proportional to γ; with these terms an analytic solution does not appear possible.

However, one can still deduce the qualitative behavior of the populations with γ. Unlike the total decay rate $\Gamma>0$, the difference γ can be positive (for $\Gamma_1>\Gamma_3$) or negative (for $\Gamma_1<\Gamma_3$). It is clear from Eq. (38) that the solution is not

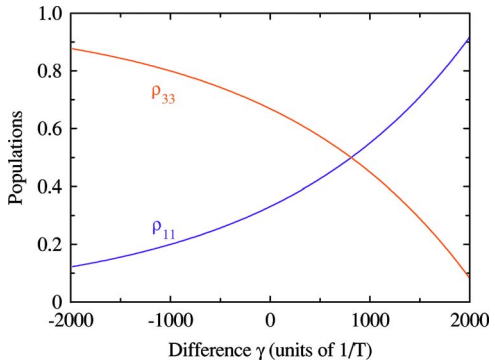

FIG. 5. (Color online) Numerically calculated final-state population ρ_{33} plotted against the difference $\gamma=\Gamma_1-\Gamma_3$ of the decay rates of state $|2\rangle$ to states $|1\rangle$ and $|3\rangle$. We have assumed Gaussian pulse shapes (28) with pulse delay $\tau=1.5T$, peak Rabi frequency $\Omega_0=60T^{-1}$, and total decay rate $\Gamma=2000T^{-1}$.

symmetric with respect to the sign of γ. Because $-1\leqslant w\leqslant 1$ and because $\sin 2\vartheta\geqslant 0$, the sign of the last term in Eq. (38a) is the same as the sign of γ. Furthermore, for small-to-moderate population losses (then $w<0$) the term $-2\dot{\vartheta}w>0$ because $\dot{\vartheta}>0$, see Eq. (29a). These two terms determine the effective interaction between the dark and bright state, which is responsible for the population loss from the dark state. For $\gamma<0$ the term with γ is negative and hence the interaction between $|d\rangle$ and $|b\rangle$ weakens, which should lead to smaller population loss from state $|d\rangle$ than for $\gamma=0$. On the contrary, for $\gamma>0$ the term with γ is positive and the interaction between $|d\rangle$ and $|b\rangle$ increases, which should lead to larger population loss from state $|d\rangle$. In result, the population ρ_{33} is expected to decrease as γ grows from $-\Gamma$ to Γ.

This feature is indeed seen in Fig. 5, which shows the populations ρ_{11} and ρ_{33} against the difference γ between the decay rates. A monotonic behavior is observed with ρ_{33} increasing as γ approaches $-\Gamma$ to the left. This limit corresponds to $\Gamma_1=0$ and $\Gamma_3=\Gamma$, which is obviously favorable for ρ_{33} as spontaneous emission occurs then in the desired direction, towards state $|3\rangle$. The other limit $\gamma\rightarrow\Gamma$, corresponding to $\Gamma_3=0$ and $\Gamma_1=\Gamma$, is least favorable for STIRAP, because then the spontaneous emission returns the population back to the initial state $|1\rangle$.

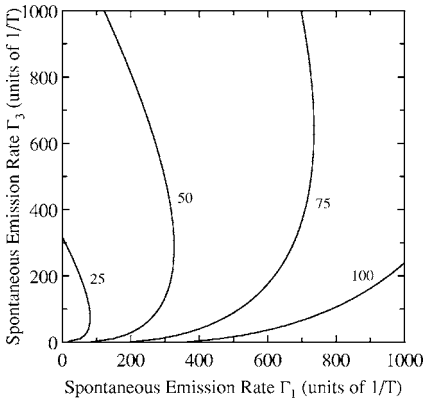

FIG. 6. Numerically calculated level lines, for which the final-state population is $\rho_{33}=0.9$, plotted against the decay rates of state $|2\rangle$ to states $|1\rangle$ and $|3\rangle$. The population ρ_{33} exceeds 0.9 on the left side of the respective curve. We have assumed Gaussian pulse shapes (28) with pulse delay $\tau=1.5T$ and four values of the peak Rabi frequency, $\Omega_0=25T^{-1}$, $50T^{-1}$, $75T^{-1}$, and $100T^{-1}$, denoted nearby the respective line.

Figure 6 shows the level lines, on which the population ρ_{33} equals 0.9, against the two decay rates Γ_1 and Γ_3. The population ρ_{33} exceeds the value 0.9 on the left of the respective line. The figure confirms the qualitative prediction that STIRAP is more sensitive to the decay rate Γ_1 since it drives the population oppositely to STIRAP, towards the initial state $|1\rangle$; this decrease occurs primarily due to deteriorated adiabaticity. The decrease of ρ_{33} with Γ_3 occurs at much larger values and it is a result of quantum overdamping.

VI. CONCLUSIONS

In this paper we have explored the effect of spontaneous emission on the population transfer efficiency in STIRAP. We have derived an approximate analytic solution to the Liouville equation, which has been verified by comparison with numerical simulations to provide a very accurate description of the populations. The solution has been derived by transforming the Liouville equation to the dark-excited-bright basis and identifying there weakly coupled populations and coherences, which have been eliminated adiabatically.

Besides providing an accurate quantitative description of spontaneous emission in STIRAP, we have found several interesting features. We have concluded that for small-to-moderate decay rates STIRAP is not affected very significantly by spontaneous emission. Then for moderate-to-strong decay rates STIRAP degenerates into incoherent pulsed OP. The definitions of "weak," "moderate," and "strong" decay rates depend on the peak Rabi frequency Ω_0 and they scale with Ω_0^2. For very strong spontaneous emission the system gets overdamped and freezes in its initial state for $\Gamma\rightarrow\infty$. These results provide quantitative estimates of the robustness of STIRAP in lossy conditions and explain why STIRAP has been implemented successfully in numerous systems even when the intermediate-state lifetime has been much shorter than the pulse duration [4].

ACKNOWLEDGMENTS

This work has been supported by the European Union's Transfer of Knowledge project CAMEL (Grant No. MTKD-CT-2004-014427), the EU Research and Training Network QUACS (Grant No. HPRN-CT-2002-00309), and Max-Planck Forschungspreis 2003. P.A.I. acknowledges support from the EU Marie Curie Training Site Project No. HPMT-CT-2001-00294. N.V.V. acknowledges support from the Alexander von Humboldt Foundation.

APPENDIX: CALCULATION OF THE INTEGRAL *F*

We estimate the integral (31) by using two approximations. *First*, we replace $\mathrm{sech}^2 x$ by a Gaussian,

$$\operatorname{sech}^2 x \approx e^{-\pi x^2/4}, \tag{A1}$$

since both functions are pulse-shaped, have the same maximum at $x=0$, and the same pulse area. *Second*, we replace the cosh factor in Eq. (31) as

$$\cosh\left\{\frac{a}{2}\left[\operatorname{erf}\left(\frac{2t-\tau}{T\sqrt{2}}\right)+\operatorname{erf}\left(\frac{2t+\tau}{T\sqrt{2}}\right)\right]\right\} \approx \cosh a-(\cosh a-1)e^{-\pi b\tau^2 t^2/T^4}, \tag{A2}$$

where a is given by Eq. (33a) and b is a free parameter. The justification is that the left-hand side is an inverted-bell-shaped function, which has a minimum of 1 at $t=0$ and tends to $\cosh a$ for $t\to\infty$; the function on the right-hand side of Eq. (A2) has the same properties but it allows the exact integration of Eq. (31). The parameter b is determined by imposing the condition that the second time derivatives of these "inverted-bells"are equal at $t=0$, which is motivated by the fact that the main contribution to the integral (31) comes from the region around $t=0$ because of the sech^2 factor; this leads to Eq. (33b).

With the replacements (A1) and (A2), the integral (31) can be solved exactly and the result is given by Eq. (32).

[1] U. Gaubatz, P. Rudecki, S. Schiemann, and K. Bergmann, J. Chem. Phys. **92**, 5363 (1990).

[2] K. Bergmann, H. Theuer, and B. W. Shore, Rev. Mod. Phys. **70**, 1003 (1998).

[3] N. V. Vitanov, T. Halfmann, B. W. Shore, and K. Bergmann, Annu. Rev. Phys. Chem. **52**, 763 (2001).

[4] N. V. Vitanov, M. Fleischhauer, B. W. Shore, and K. Bergmann, Adv. At., Mol., Opt. Phys. **46**, 55 (2001).

[5] N. V. Vitanov and S. Stenholm, Phys. Rev. A **56**, 1463 (1997).

[6] L. P. Yatsenko, V. I. Romanenko, B. W. Shore, and K. Bergmann, Phys. Rev. A **65**, 043409 (2002).

[7] Q. Shi and E. Geva, J. Chem. Phys. **119**, 11773 (2003).

[8] P. A. Ivanov, N. V. Vitanov, and K. Bergmann, Phys. Rev. A **70**, 063409 (2004).

[9] R. Garcia Fernandez, A. Ekers, L. P. Yatsenko, N. V. Vitanov, and K. Bergmann, Phys. Rev. Lett. **95**, 043001 (2005).

[10] B. W. Shore, *The Theory of Coherent Atomic Excitation* (Wiley, New York, 1990).

[11] N. V. Vitanov and S. Stenholm, Opt. Commun. **135**, 394 (1997).

[12] L. Allen and J. H. Eberly, *Optical Resonance and Two-Level Atoms* (Dover, New York, 1987).

[13] M. Abramowitz and I. A. Stegun, *Handbook of Mathematical Functions* (Dover, New York, 1964).